



Hydration kinetics and activation energy of cement pastes containing various nanoparticles

Yogiraj Sargam, Kejin Wang*

Iowa State University, Department of Civil, Construction, and Environmental Engineering, 813 Bissell Road, Ames, IA, 50011, USA

ARTICLE INFO

Keywords:
Portland cement
Nanoparticles
Filler effect
Hydration kinetics
Activation energy

ABSTRACT

The relative effects of nanoparticles (NPs) of dry powdered nSiO₂, nAl₂O₃, and nCaCO₃ and colloidal nSiO₂ (in size range of 10–40 nm) on the hydration kinetics and apparent activation energy (E_a) of Portland cement were analyzed. Different variables, such as NP replacement levels (0, 0.5, and 5 wt %) and testing temperature (10–40 °C), were evaluated. For a given type of NPs, the acceleration effect on cement hydration increased with increasing NP replacement level, but it reduced with increasing testing temperature. Apparent E_a increased at low replacement while it reduced at high replacement level of NPs, which was thought to occur due to an enhanced reduction in the rate of diffusion-control hydration at high replacement level. Accounting for the specific surface areas (SSA) of cement and NPs, the filler effect of NPs was quantified in terms of area multiplier. It was revealed that a NP with high SSA could function as a better accelerator at low replacement than the one with low SSA at high replacement. For tailoring the setting and strength development behavior of cementitious systems, the results from this study can aid in an informed decision making for the selection of the type of NP and its dosage. Moreover, the apparent E_a values can be used for the maturity prediction of nanoengineered cementitious composites.

1. Introduction

The inclusion of nanosized particles (NPs) in a cementitious system is gaining increasing attention. Owing to their fine particles and high surface area-to-volume ratio, NPs show high surface reactivity and provide nucleation sites for C-S-H gel to grow, thus accelerating cement hydration [1–4]. Due to their filler effect, NPs enhance the packing density of cementitious systems, thus reducing the porosity of the hardened products [2,5–10]. Also, NPs can immobilize free water in cementitious systems, thus improving the properties of the interfacial transition zone (ITZ) between the cement matrix and aggregate [11–17]. Different types of NPs are used as additives or replacement materials for cement. In general, these are classified as zero-dimensional (0D), one-dimensional (1D), and two-dimensional (2D) materials based on their geometries. NPs, such as nanosilica (nSiO₂), nanotitanium dioxide (nTiO₂), nanoalumina (nAl₂O₃), nanolimestone (nCaCO₃), and others, fall into the category of 0D. At the same time, carbon nanotubes (CNTs) and nanofiber are categorized as 1D nanomaterials, and graphene and graphene oxide are classified as 2D nanomaterials [18].

The setting behavior and strength development of a cementitious

system are dependent on its hydration kinetics, which in turn depends on the chemical and physical properties of the cementitious materials. The presence of reactive and nonreactive additives and admixtures, as well as different curing temperatures, can also alter the rate of cementitious hydration significantly. Therefore, the knowledge of the temperature sensitivity and apparent activation energy (E_a) of cementitious systems with various supplementary cementitious materials (SCMs) and additives is essential for understanding the time-dependent behavior of the cement-based materials.

E_a is the potential energy barrier between the reactant and product for a single reaction system. Cement hydration generally consists of a complicated set of reactions, each of which has its own E_a , and therefore, to account for the composite nature of these reactions, the term apparent E_a is employed in the case of cement hydration [19]. Apparent E_a has been widely used in calculations of concrete maturity or equivalent age, which directly connects concrete strength with its heat generation and age. For example, for a cementitious system with an apparent E_a of 40 kJ/mol, curing a concrete specimen for 12 h at 40 °C is equivalent to curing for 26 h at 25 °C [19]. Another application of apparent E_a is for the prediction of temperature development in a mass concrete member

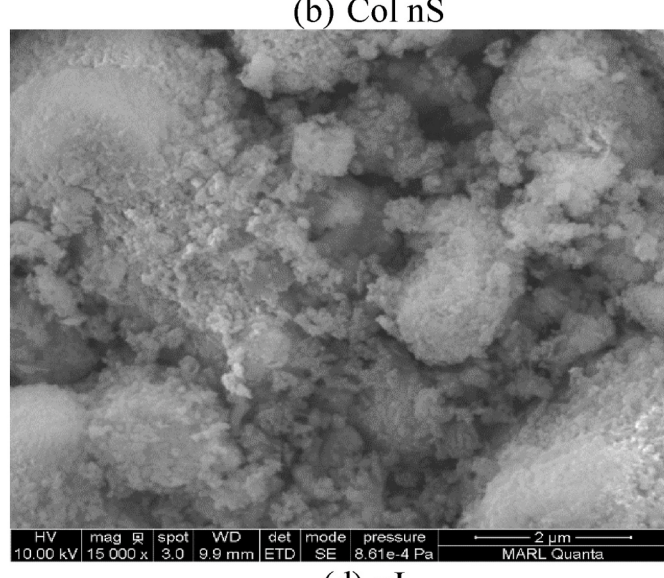
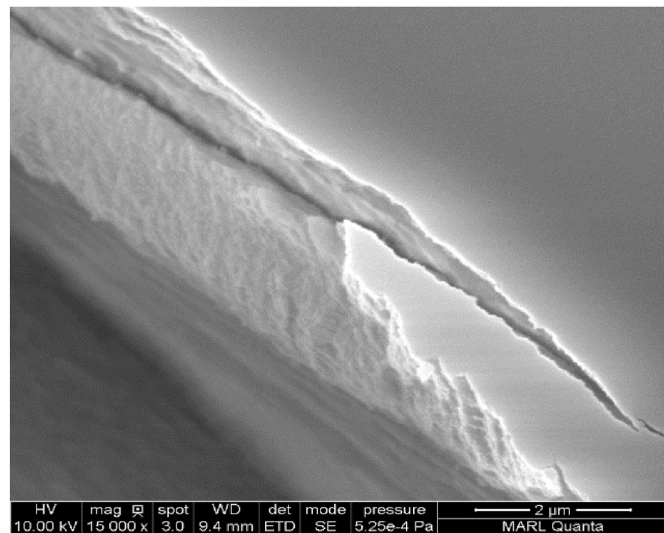
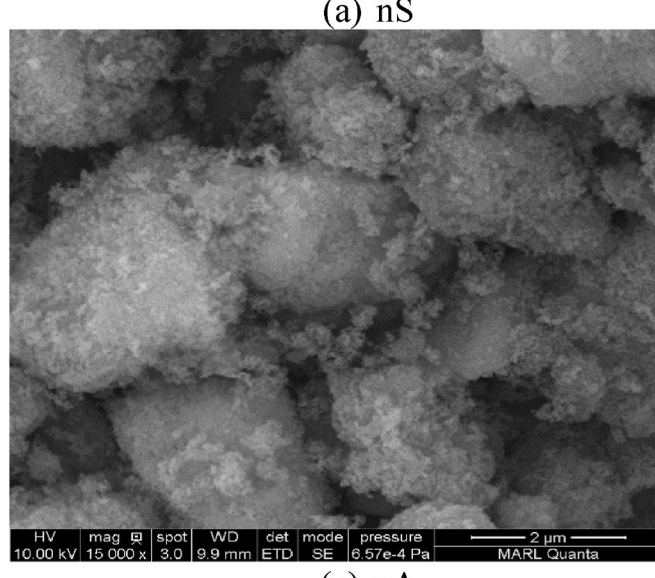
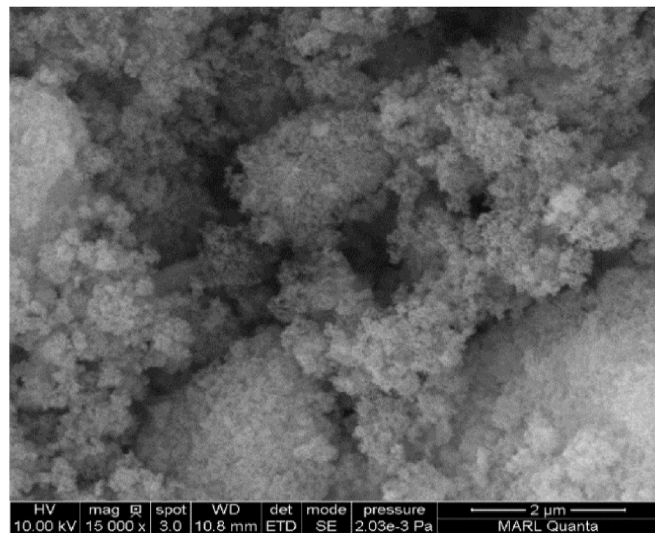
* Corresponding author.

E-mail addresses: ysargam@iastate.edu (Y. Sargam), kejinw@iastate.edu (K. Wang).

Table 1

Properties of materials used in this study.

Material	Source	Avg. particle size (nm)	Specific surface area (m^2/g)	Density (g/ml)	pH	Purity (%)	Solids content (%)
Cement (Type I/II)	Ash Grove	~35000	0.44	–	–	–	–
nSiO ₂ (nS)	Aldrich	10–20	~200	2.17–2.66	–	99.5	–
Colloidal nSiO ₂ (Col nS)	Nouryon Levasil CB25	10–20	~225	1.209	10.4	–	30
nAl ₂ O ₃ (nA)	SkySpring Nanomaterials	20	~100	3.5–3.9	–	99.9	–
nCaCO ₃ (nL)	SkySpring Nanomaterials	15–40	>40	0.680	8–9	>94.5	–

**Fig. 1.** SEM images of nanoparticles.

[20,21].

Various experimental methods, such as isothermal calorimetry [19, 22–25] and differential scanning calorimetry [26], have been proposed for determining the apparent E_a of the complex cement hydration reaction. Isothermal calorimetry (IC) is the most widely used one. Using IC, the rates of heat at different temperatures can be captured, and apparent E_a can be determined with the application of the Arrhenius equation. Poole et al. [24] discussed various approaches for determining E_a using IC.

Research has evidenced that when SCMs and chemical admixtures are included in the cementitious system, the hydration reactions, their rates, and apparent E_a of the system are all altered. For example,

apparent E_a decreases upon substitution of cement with class F fly ash and silica fume [25], whereas it is increased by slag substitution [27]. Similarly, since NPs affect hydration kinetics, they might also change E_a and, consequently, the setting and strength development characteristics of cement. Substantial research has been conducted to evaluate the performance of cementitious materials engineered with NPs in terms of their fresh properties [28–32], microstructure [8,33–36], physio-mechanical properties [37–42], and durability [37,43–45]. Several studies [28,46–50] have also focused on the effects of various NPs on the hydration characteristics of cement. However, the studies are minimal, and the relative effects of different NPs and at different replacement levels have not been investigated. Also, the temperature

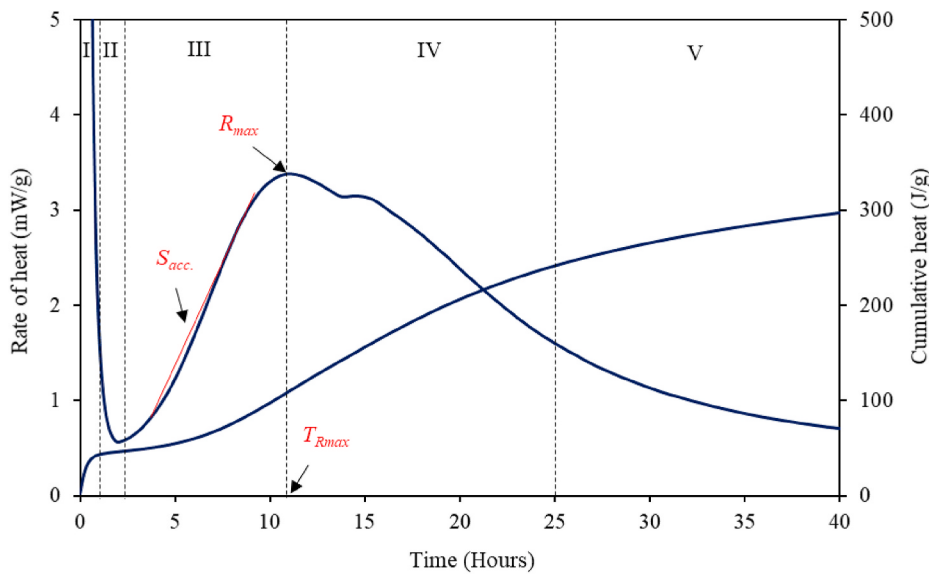


Fig. 2. A typical calorimetry curve of Portland cement hydration.

sensitivity and apparent E_a of cement in the presence of various NPs have not been thoroughly studied. Jayapalan et al. [51] performed such a study, but it was limited only to two NPs – nTiO₂ and nCaCO₃, and the filler effect of the NPs was not quantified.

In light of the above discussions, the present study analyzed the effects of NPs (dry powdered nSiO₂, nAl₂O₃, and nCaCO₃ and colloidal nSiO₂) on hydration kinetics and apparent E_a of a cementitious system. Two levels of NP replacement for cement were considered: 0.5% (low) and 5% (high). The heat of hydration was measured using IC. The apparent E_a was calculated using the two methods - single linear approximation and modified ASTM C1074. The hydration parameters and apparent E_a were also explained in terms of the area multiplier that considers the filler effect based on the specific surface areas of various NPs. The contents presented in this study are expected to provide a better understanding of the hydration kinetics, apparent E_a , and filler effect of the nanoengineered cementitious composites. In cases where a choice of these NPs is available for nanoengineering of cementitious composites, an informed decision can be made based on the results from this study. The composite can be tailored to achieve a desirable setting and early-age strength development behavior. Apparent E_a values calculated in this study can be used to determine the equivalent age of composites based on which the decision to strip the formwork can be taken.

2. Materials and methods

2.1. Materials

Type I/II Portland cement satisfying ASTM C150 [52] criteria was used for all pastes studied. The NPs used were nSiO₂, nAl₂O₃, and nCaCO₃, in powder form, which will be written as nS, nA, and nL, respectively, from now on. To compare with the powder nS, colloidal SiO₂ (Col nS), in a liquid form, was also studied. The properties of these materials are presented in Table 1.

To learn their morphology and aggregation state, the NPs, as they were received, were examined under a scanning electron microscope (SEM). A field-emission SEM, FEI Quanta 250, was used for this purpose that offered a maximum resolution on the order of 1.0 nm. An accelerating voltage of 10 kV was applied. To prepare for SEM samples, the powder NPs were dusted on their sample holders, while for Col nS, a small droplet was placed on a sample holder, which was stored in a can to let the water evaporate. All the samples were then coated with a layer

of 2-nm Iridium before being observed under SEM. Fig. 1 shows the secondary electron images (SEI) of the NPs at the 15000 \times magnification. It can be observed from Fig. 1 that all four NPs studied had a spherical shape. However, due to their fine sizes, high surface areas, and energies, attractive van der Waals forces had made the NPs form clusters of agglomerates up to the orders of 2 μ m. Comparing Fig. 1(a) (nS sample) and Fig. 1(b) (Col nS sample), one can notice that the nS sample contained various sizes of particles, including large agglomerates, while the Col nS sample showed densely packed NPs with uniform particle size. This is because the original colloidal solution contained well dispersed NPs. Therefore, the ultrasonication technique was used to break up the agglomerates in the powder NPs before the NPs were introduced into a cement system; however, the ultrasonication was not used for the Col nS.

2.2. Methods

2.2.1. Preparation of the cement-NP paste

This section describes the procedure used for the preparation of cement paste containing NPs (cement-NP paste). To prepare a cement-NP paste, the quantities of the necessary constituents (cement, NP, and water) were firstly determined. All pastes were designed to have a water-to-binder ratio (w/b) of 0.45. The quantity of NPs was set as 0% (control), 0.5% and 5% (by weight) of replacement for cement. With the determined quantity of the NPs and water, a nanosolution was prepared by dispersing the NPs in the water using a probe-based ultrasonication technique. A ½ inch probe ultrasonicator (MISONIX Incorporated model XL2020) having an output frequency of 20 kHz and generating power of 600W was used. The ultrasonication for each nanosolution was performed for 30 min in a 5-s pulse on and 1.5-s pulse off mode (The time of the ultrasonication was determined from a separate study). During the entire ultrasonication period, the vial containing the nanosolution was kept in an ice-water bath to avoid the overheating of the sample. The ultrasonicated nanosolution was then used as ‘mixing water’ for the preparation of the paste by 2 min of hand-mixing. When Col nS was used, the amount of the water present in the colloid was deducted from the mixing water calculated for the paste. Since the NPs were already dispersed in the aqueous solution, ultrasonication was not applied. The Col nS solution was used directly as a part of ‘mixing water’ for its paste.

2.2.2. Isothermal calorimetry

After the completion of mixing, approximately 25 g of paste was

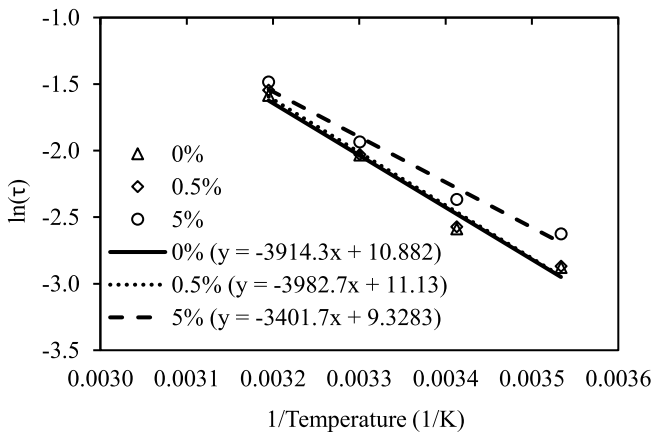


Fig. 3. Arrhenius plot for calculation of E_a (paste containing nS).

placed into an aluminum sample holder and tested for the rate of the heat of hydration using an isothermal calorimeter. A PTC-1 calorimeter was used that measured the rate of heat at a constant temperature following ASTM C1679 [53]. The calorimeter contains eight separate channels. During a test, each channel held a sample that rested on a heat flow sensor (Peltier), which was positioned on a standard heat sink of a large block of aluminum. Proportional to the amount of heat flow, a voltage signal was recorded at fixed intervals (2-min in this study). The voltage was then converted to the rate of heat generation by applying the calibration factor based on the reference material (aluminum). In this study, the calorimetry measurements were performed for each cement-NP paste at four constant temperatures (10, 20, 30, and 40 °C), and two samples were tested at each of the temperatures. A typical

calorimetry curve of Portland cement hydration is shown in Fig. 2 with the rate of heat generation plotted on the primary y-axis and the cumulative heat on the secondary y-axis. In order to compare the effects of various NPs used in this study, four parameters from the calorimetry curve (Fig. 2) were used as follows:

- (1) The maximum rate of heat generation (R_{max}): higher value means that alite hydrates at a higher rate
- (2) Time to reach the maximum rate of heat generation (T_{Rmax}): a lower value suggests the acceleration of hydration
- (3) The slope of the acceleration region ($S_{acc.}$): a higher value means a higher rate of cement hydration in the acceleration period. It was calculated as the slope of the linear regression line through the data points between the point where the rate of hydration starts accelerating to the point where it peaks.
- (4) Cumulative heat at a time t (H_t): a higher value suggests a higher degree of hydration at time t

According to Bullard et al. [54], the rate of heat curve can be divided into five different stages. *Stage I* – dissolution stage: A very high peak of heat is observed in this stage due to the fast dissolution of ionic phases. *Stage II*: This stage is characterized by a period of slow chemical activity and is called the induction period. Many theories, such as protective membrane, nucleation and growth (N+G), and geochemical theory, have been proposed to explain the activities in this period. According to the N+G theory [54,55], the hydration kinetics in the induction period is controlled by the nucleation and growth of CSH. When CSH nuclei reach a critical number and size, they start growing, leading to the acceleration period (Stage III). *Stage III*: This stage corresponds to the acceleration of hydration, leading to the main peak. In this period, the hydration kinetics is controlled by the N+G of hydrates, especially CSH on the surface of alite and other minerals [54,55]. The researchers have found

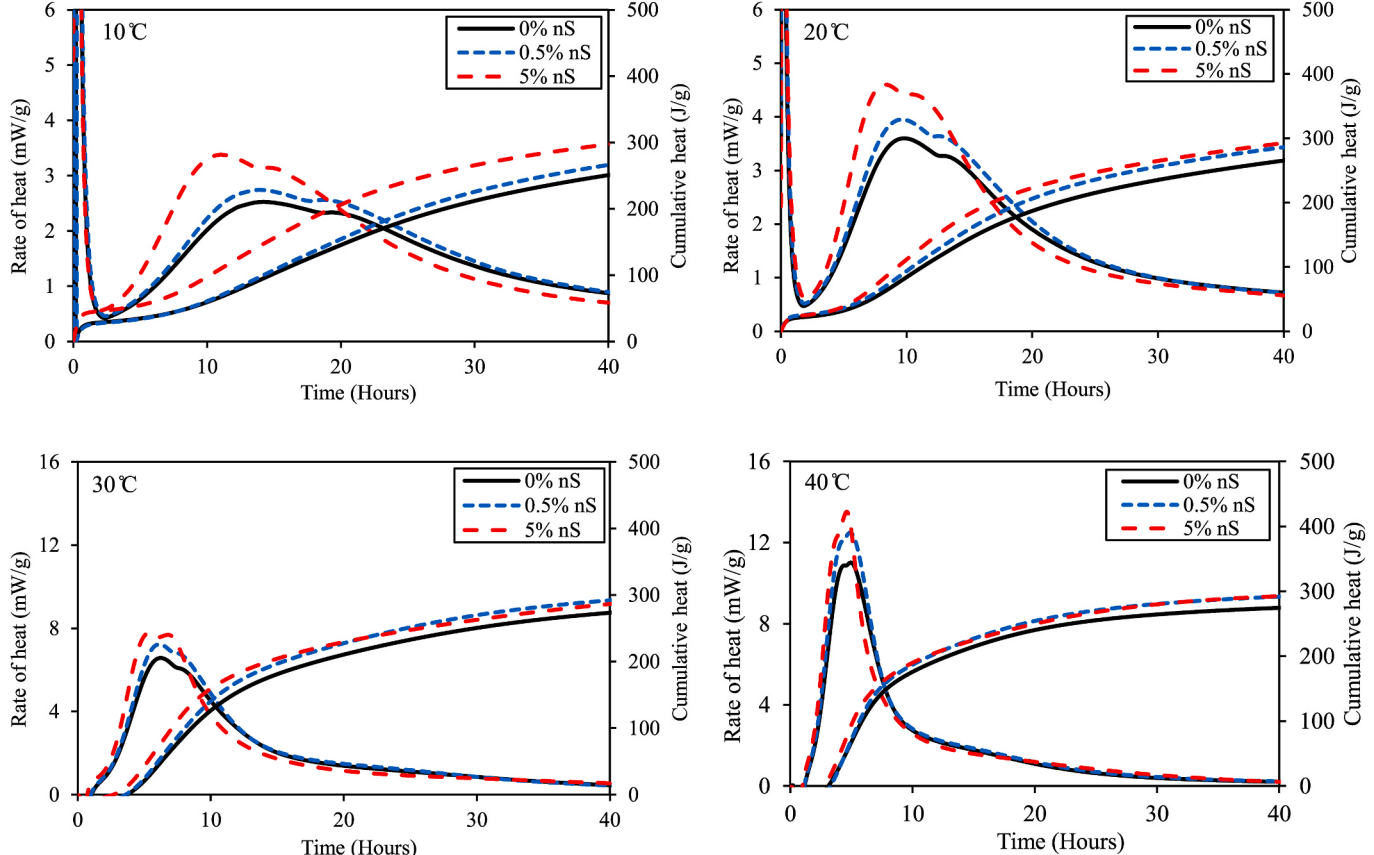


Fig. 4. Rate of heat generation and cumulative heat profiles of cement paste with nS.

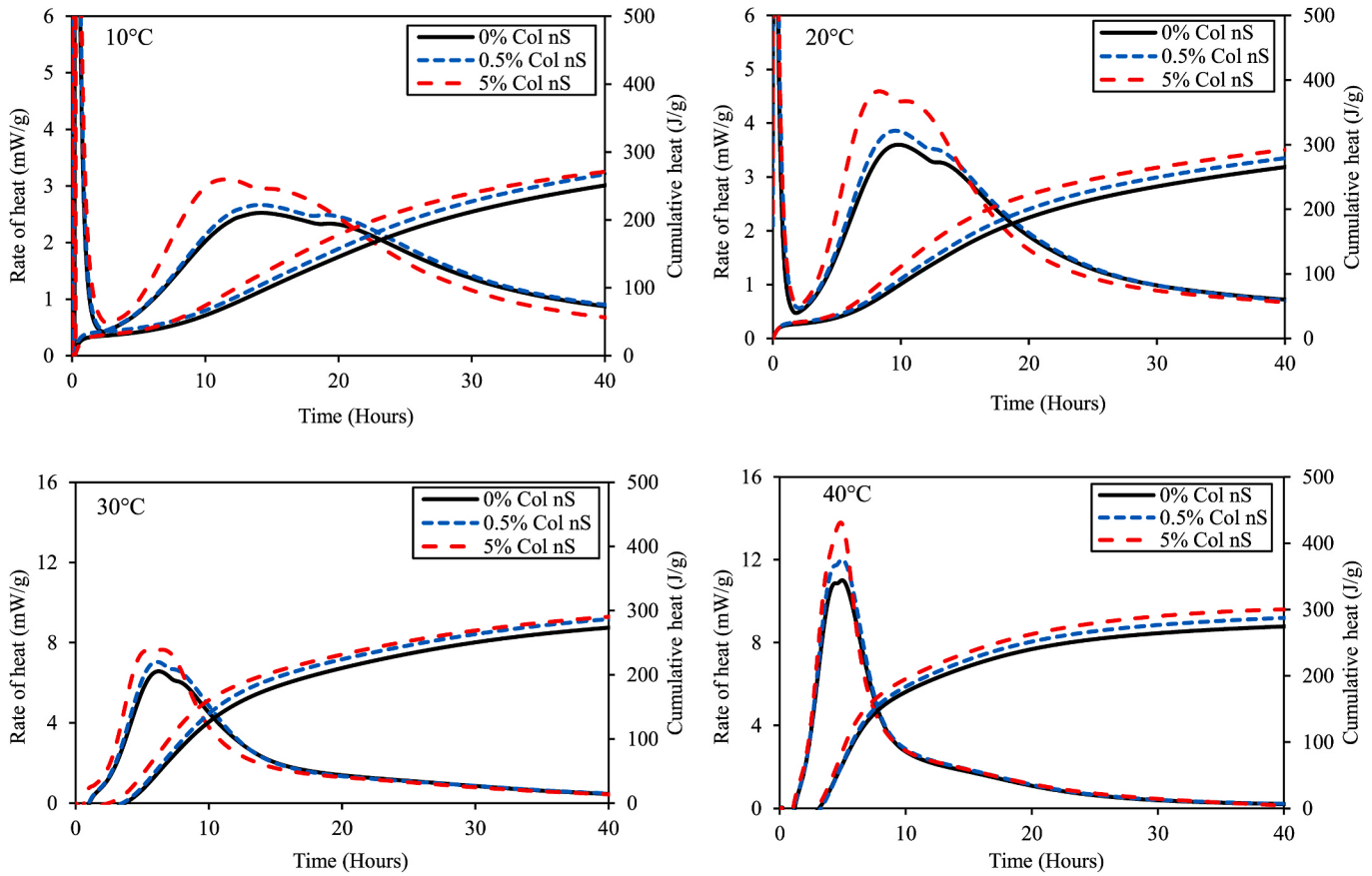


Fig. 5. Rate of heat generation and cumulative heat profiles of cement paste with Col nS.

that the rate of hydration is proportional to the number of active growth sites for CSH [54]. *Stage IV:* This stage corresponds to the deceleration of cement hydration. Although different explanations have been given, it is widely considered that this period is controlled by the diffusion process. As the unhydrated grains are covered by the CSH rim around them, the rate of hydration is controlled by how fast or slow the ions can diffuse through these rims [56]. However, this step is affected by several other factors such as lack of water, particle size and SSA of reactants, and consumption of small particles leaving only large particles to react [54]. *Stage V:* After around 24 h (Stage V), the chemical activity occurs very slowly, which depends on the space available for the cement hydrates. The growth of hydrates until stage IV heavily restricts the diffusion of ions, thereby limiting further hydration of unhydrated grains. In other words, this period is also diffusion controlled.

2.2.3. Method of E_a calculation

As mentioned previously, various methods have been proposed for determining the temperature sensitivity and calculating E_a of cementitious materials [19,22–25] using the isothermal calorimetry data. Poole et al. [24] presented three such popular methods along with their advantages and disadvantages. These methods were (1) single linear approximation, (2) incremental, and (3) modified ASTM C1074. In this study, single linear approximation, and modified ASTM C1074 methods were employed. In the linear approximation method, the linear slope of the acceleratory region of the cumulative heat curve (developed from the isothermal calorimetry measurements at different temperatures) was considered as the rate of reaction. The rates of reaction at different temperatures were then used to calculate E_a through the Arrhenius equation. As per the modified ASTM C1074 method, E_a was calculated through the following steps:

(1) Rate of heat (normalized in mW/g of cementitious materials) data were obtained for each cement-NPs combination by isothermal calorimetry measurements separately at four temperatures: 10, 20, 30, and 40 °C. The cumulative heat was also calculated using this data.

(2) The development of the degree of hydration (DOH) with time was calculated using Eqs. (1)–(3) [25,57,58].

$$\alpha(t) = \frac{H(t)}{H_u} \quad (1)$$

$$H_u = H_{cem} \cdot p_{cem} + H_{nS} \cdot p_{nS} + H_{nA} \cdot p_{nA} + H_{nL} \cdot p_{nL} \quad (2)$$

$$H_{cem} = 500 \cdot p_{C_3S} + 260 \cdot p_{C_2S} + 866 \cdot p_{C_3A} + 420 \cdot p_{C_4AF} + 624 \cdot p_{SO_3} \\ + 1186 \cdot p_{FreeCa} + 850 \cdot p_{MgO} \quad (3)$$

Where $\alpha(t)$ is the DOH at time t ; $H(t)$ is the cumulative heat at time t , and H_u is the total heat available for the reaction. H_{cem} , H_{nS} , H_{nA} , and H_{nL} in Eq. (2) represent the total heat available due to reaction of cement, nS (both powder and colloidal), nA, and nL, respectively. H_{cem} is calculated based on the chemical composition of cement as per Eq. (3) wherein the heat generated due to various cement compounds such as C_3S , C_2S , C_3A , and others were considered separately. As both nS and nA were reactive NPs, the values of H_{nS} and H_{nA} were considered as 780 J/g and 230 J/g, respectively, based on previous studies [59]. On the other hand, nL was less reactive, and it was assumed an inert filler [47,51] in the present study for simplicity, and hence H_{nL} was considered to be zero. p_{cem} , p_{nS} , p_{nA} , and p_{nL} in Eq. (2) represent the percentage of cement, nS (powder and colloid), nA, and nL in the paste, respectively.

(3) The DOH calculated in step 2 was modeled using the three-parameter model given in Eq. (4).

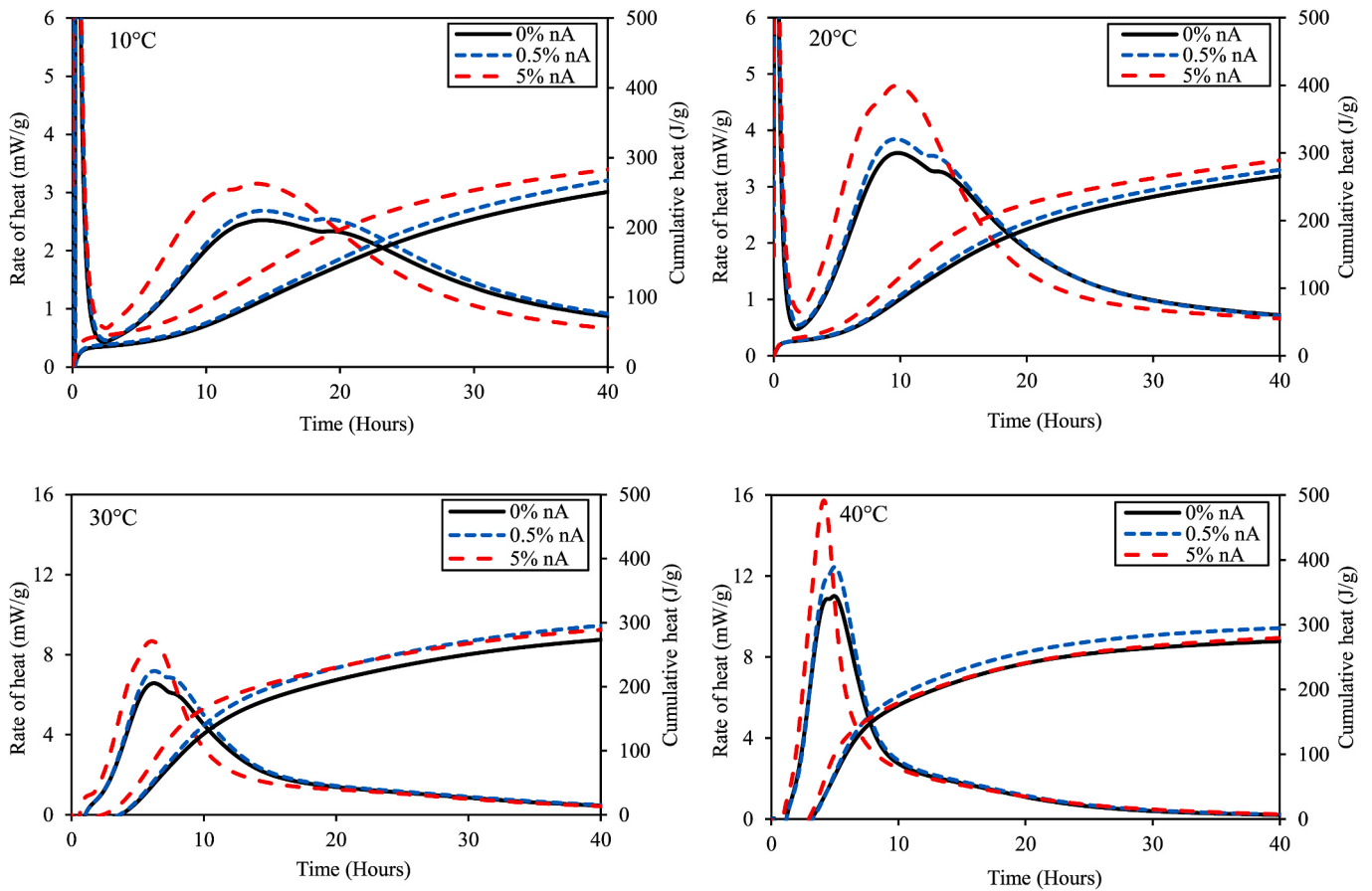


Fig. 6. Rate of heat generation and cumulative heat profiles of cement paste with nA.

$$\alpha(t) = \alpha_u \cdot e^{-\left[\frac{t}{\tau}\right]^\beta} \quad (4)$$

Where the three coefficients, α_u , β , and τ , are the ultimate DOH, hydration shape parameter, and hydration time parameter, respectively. A larger α_u indicates the higher magnitude of ultimate DOH, larger β indicates a higher hydration rate at the linear portion of the hydration curve, and a larger τ means a more significant delay of hydration [60]. By fitting DOH data using a least-squares approach, the three coefficients of the model were obtained at each of the four temperatures. It has been shown in the literature that α_u and β are independent of temperature [25,61]. Therefore, keeping the values of α_u and β constant (equal to their values at 20°C), the value of τ was re-calculated at each temperature.

(4) $\ln(\tau)$ versus 1/Temperature (K) was plotted using Eq. (5).

$$E_a = - \frac{\ln\left(\frac{\tau_{ref}}{\tau_c}\right)}{\left(\frac{1}{T_{ref}} - \frac{1}{T_c}\right)} \cdot R \quad (5)$$

Where τ_{ref} and T_{ref} are hydration time parameter and cement paste temperature at the reference temperature (20°C); τ_c and T_c are hydration time parameter and cement paste temperature at different temperatures, and R is the natural gas constant.

(5) The value of E_a was then calculated as the slope of the best-fit line times the negative of R (8.314 J/mol/K). For example, the calculation of E_a for 0%, 0.5%, and 5% of dry powder nS is shown

in Fig. 3. It can be observed that as the slope of the best-fit line changes, the value of E_a will also change.

3. Results and discussion

3.1. Effect of NPs on cement hydration

3.1.1. Effect of NP replacement level

Figs. 4–7 present the heat of hydration curves from calorimetric tests of all cement-NP pastes studied. The major peaks seen in the heat of hydration curves resulted mainly from the hydration of C_3S of Portland cement. It can be seen from Figs. 4–7 that regardless of the NP type, the rate of heat generation and the total cumulative heat of all pastes studied increased, but the time to reach the max. rate of heat generation was shortened with increasing NP replacement level. This suggests that NP replacement for cement increased rate and degree of cement hydration. The shortened time to reach the max. rate of heat generation provided by NP replacements reflects a reduced set time of the cement-NP paste. Generally, at a low replacement level (0.5%), the values of the changes (increases or decreases) in the heat generation parameters studied were minimal. However, at a high replacement level (5%), they were significant. The changes in the heat generation parameters appeared more substantial for pastes tested at a low temperature when compared with those of pastes tested at a high temperature. To further understand these observations, the effects of NP replacement levels on four parameters of the heat of hydration curve were examined: (1) the maximum rate of heat generation (R_{max}); (2) the time to reach the max. rate of heat generation (T_{Rmax}); (3) the slope of the acceleration region ($S_{acc.}$); and (4) the cumulative heat at 24 h ($H_{24\text{h}}$). The cumulative heat at 24 h was chosen for comparison since the main hydration peak was finished in all cement-NP paste by this time. An example of the change in the four

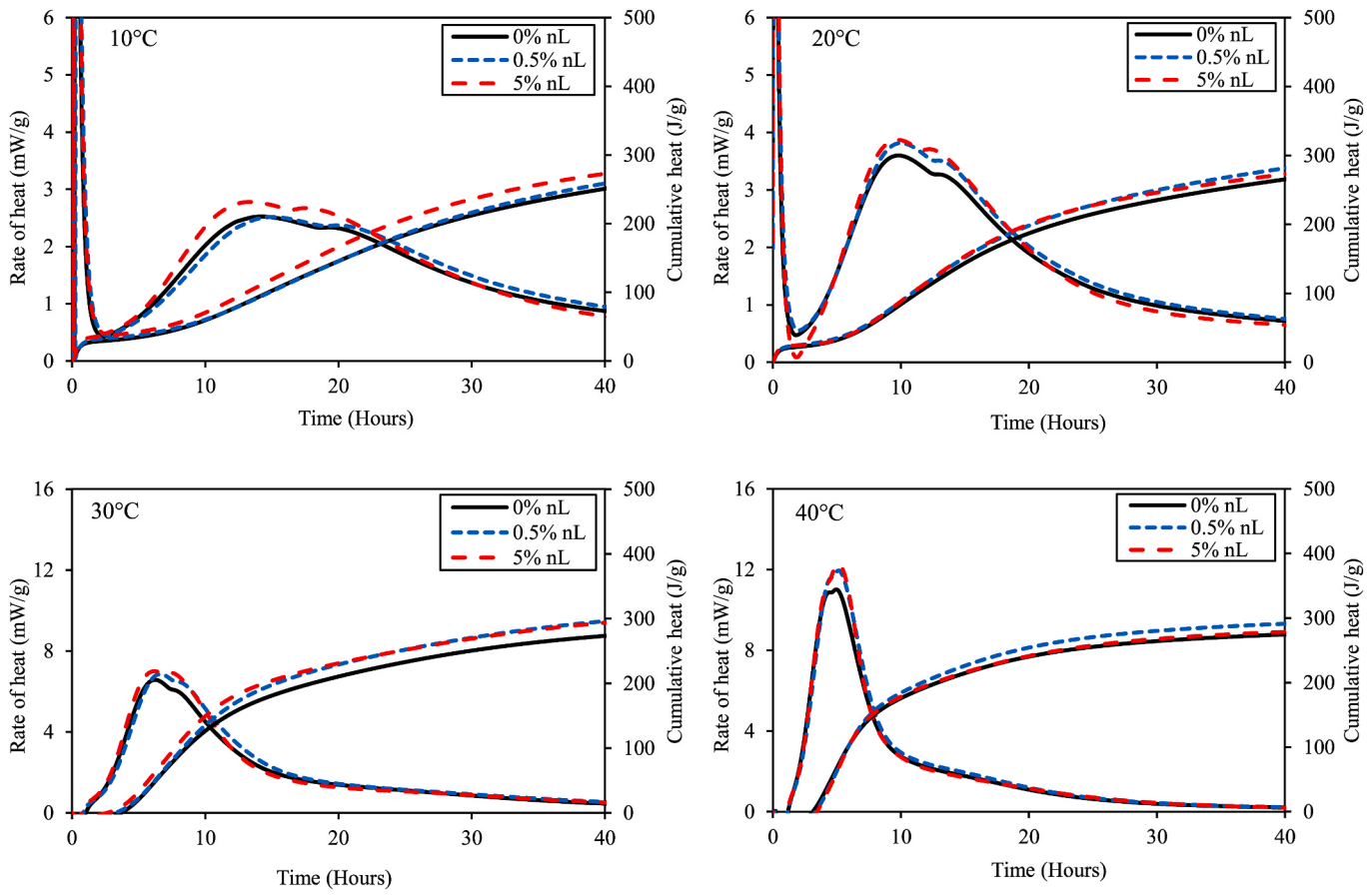


Fig. 7. Rate of heat generation and cumulative heat profiles of cement paste with nL.

parameters with nS replacement level at different temperatures is shown in Fig. 8. It can be observed that with an increase in the nS replacement level, R_{max} , S_{acc} , and $H_{24\text{ h}}$ increased, and T_{Rmax} reduced. For example, at 20°C, R_{max} increased from 3.60 mW/g to 4.60 mW/g as nS replacement level was increased from 0% to 5%. A corresponding reduction in T_{Rmax} was from 9.85 h (591 min) to 8.12 h (487 min), suggesting a significant acceleration of the hydration. Similar observations were also made in the case of other types of NPs. These observations can be attributed to the seeding effect of the NP in the cementitious system. In the presence of NPs, the seeding effect alters the kinetics in different stages of cement hydration with more significant effects on the induction and acceleration period (Stage II and III in Fig. 2). Shortly after mixing of a cement paste, the nuclei of the main hydration product, CSH gel, begin to form at the surfaces of the C₃S particles. The nucleation rate depends on the surface area of the particles, Ca²⁺ concentration in the solution, and the temperature [4,62]. Also, the formation of the CSH gel is autocatalytic, which implies that the existing CSH NPs stimulate the nucleation of new particles. A continuous autocatalytic process further triggers their growth as well [4]. Similar to this concept, the inclusion of NP seeds, such as nS, nA, and nL, provides additional sites for the nucleation and growth (N+G) of CSH and other hydration products. This is called the seeding effect due to which two N+G processes might occur at the same time: (1) the natural heterogeneous N+G of the hydration products at particle surfaces; and (2) additional heterogeneous N+G in the capillary pore space between the particles away from the surfaces where the seeds do not affect the dissolution of C₃S [17]. As a result of the increase in NP nucleation seeding (i.e., increase in NP replacement level), three main alterations in the cement hydration could be observed [4] as follows:

- (1) a higher increment of the early rate and the peak rate [increase in R_{max} in Fig. 8(a)] since an enhanced number of regions of hydration products grow simultaneously.
- (2) significant shortening of the induction period [reduction in T_{Rmax} and increase in S_{acc} in Fig. 8(b-c)] as a large number of nuclei become available for N+G right after mixing.
- (3) a higher degree of hydration during the early N+G period [increase in $H_{24\text{ h}}$ in Fig. 8(d)] since the growth of additional hydration products in the capillary pores would not immediately cover the C₃S particles and, therefore, would not hinder the diffusion of ions.

In summary, providing additional nucleation sites, the high level of NP replacement could help accelerate the early hydration, shorten the induction period, and increase the total amount/degree of hydration at the early age, as observed in this study.

3.1.2. Effect of temperature

The hydration kinetics of cement is substantially affected by the changes in temperature, and the inclusion of NP could further affect it. To evaluate this, the rate of heat and the cumulative heat curves for cement-NPs pastes were plotted at the four tested temperatures. Since all cement-NP pastes exhibited a similar pattern, only an example of curves obtained in the case of nS is shown in Fig. 9. The following observations can be made from the figure as the testing temperature increased: (1) the dormant period reduced, suggesting faster setting of the paste at high temperatures, (2) the main hydration peak and the sulfate depletion peak shifted towards left to earlier hydration times, and (3) higher cumulative heat was released, suggesting a higher degree of hydration at early-age (around 24 h) of the paste. These can also be understood from Fig. 8 as with an increase in temperature, R_{max} , S_{acc} , and $H_{24\text{ h}}$ increased,

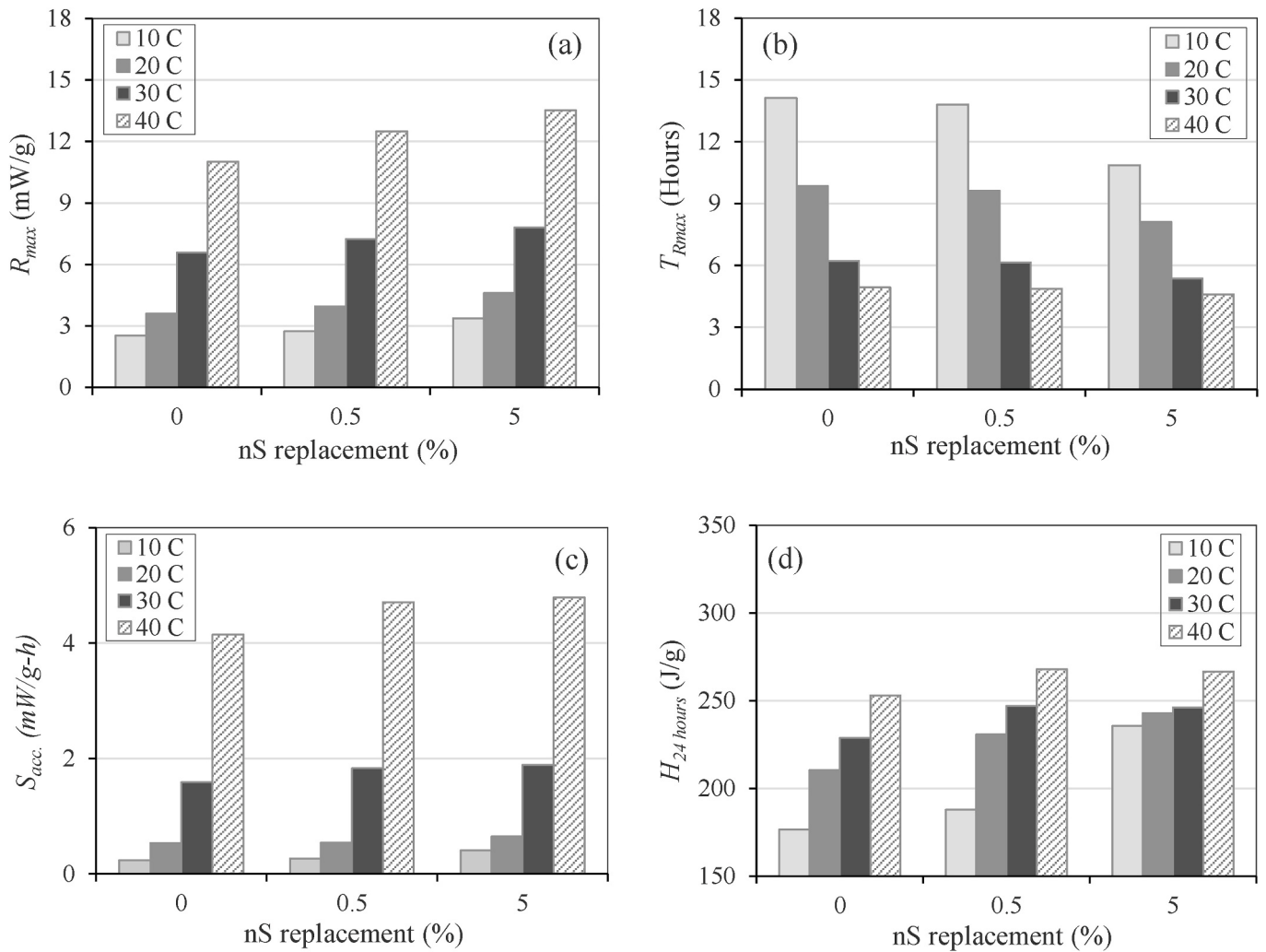


Fig. 8. Effect of NP replacement level on the hydration curve parameters (Example of nS).

and T_{Rmax} reduced at all levels of NP replacement. However, combining the effects of both NP and temperature, it was observed that increasing NP replacement level had a more prominent effect at low temperatures than at high temperatures. In other words, the changes (increment or reduction) in the hydration parameters were more substantial for pastes tested at 10 and 20 °C when compared with those of pastes tested at 30 and 40 °C. For example, for the cement paste containing 5% nS, T_{Rmax} at the testing temperatures of 10, 20, 30, and 40 °C were approximately 11, 8, 5.5, and 4.5 h, respectively, while for the control paste sample (no NPs), the corresponding values of T_{Rmax} were 14, 10, 6, and 5 h, respectively. Similarly, T_{Rmax} values in the case of 5% Col nS were 11.5, 8, 5.9, and 4.8 h, respectively, at 10, 20, 30, and 40 °C. These results suggest that the hydration-accelerating effect of NPs was more substantial at low temperatures, and is reduced with increasing temperature, which is consistent with that observed by other researchers [51, 62]. This phenomenon can be explained by the N+G hypothesis of cement hydration products, as explained earlier. For the control paste (no NPs), cement hydration accelerates at a high temperature because the dissolution of the anhydrous cement and the precipitation of hydrates proceed faster at high temperatures [16]. The inclusion of NPs provides additional sites for N+G of hydration products; however, its rate is also dependent on the temperature, among other factors such as the surface area of the particles and Ca^{2+} concentration in the solution [4, 62]. By modeling the kinetics of C_3S hydration with a mathematical boundary N+G model, Thomas et al. [62] found that the nucleation rate has a strong nonlinear temperature dependence. He further

hypothesized that the nucleation rate increases rapidly with the temperature at lower temperatures, but it levels off at higher temperatures. This hypothesis explains well the observations from this study that the effect of NPs on the hydration kinetics are more prominent at lower temperatures. More reasons behind this observation are evident from the activation energy results, as discussed later in section 3.2.

3.1.3. Effect of NP types

In order to evaluate the effect of the type of NPs, the four parameters of the hydration curve were compared from Figs. 4–7. The percentage change (increment or reduction) in the absolute value of parameters (R_{max} , T_{Rmax} , $S_{acc.}$, and $H_{24\text{ hours}}$) for cement-NP paste were calculated with respect to its value in the case of control cement paste. Following observations were made:

- (1) For all types of NPs except nL, the percentage increase in R_{max} was higher at 5% replacement level than that at 0.5% at all temperatures, which was consistent with observations presented in sections 3.1.1 and 3.1.2. In general, considering both replacement levels and all temperatures, the order of percentage increase in R_{max} was: nA > nS > Col nS > nL. Contrary to other NPs, nA exhibited a very high increase (~40% at 40 °C) in R_{max} at 5% replacement level. Such behavior might be attributed to the high reactivity of nA particles in the alkaline environment of cement paste. Recently, Zhan et al. [63] reported that nA could accelerate not only the silicate phase but also aluminate phase

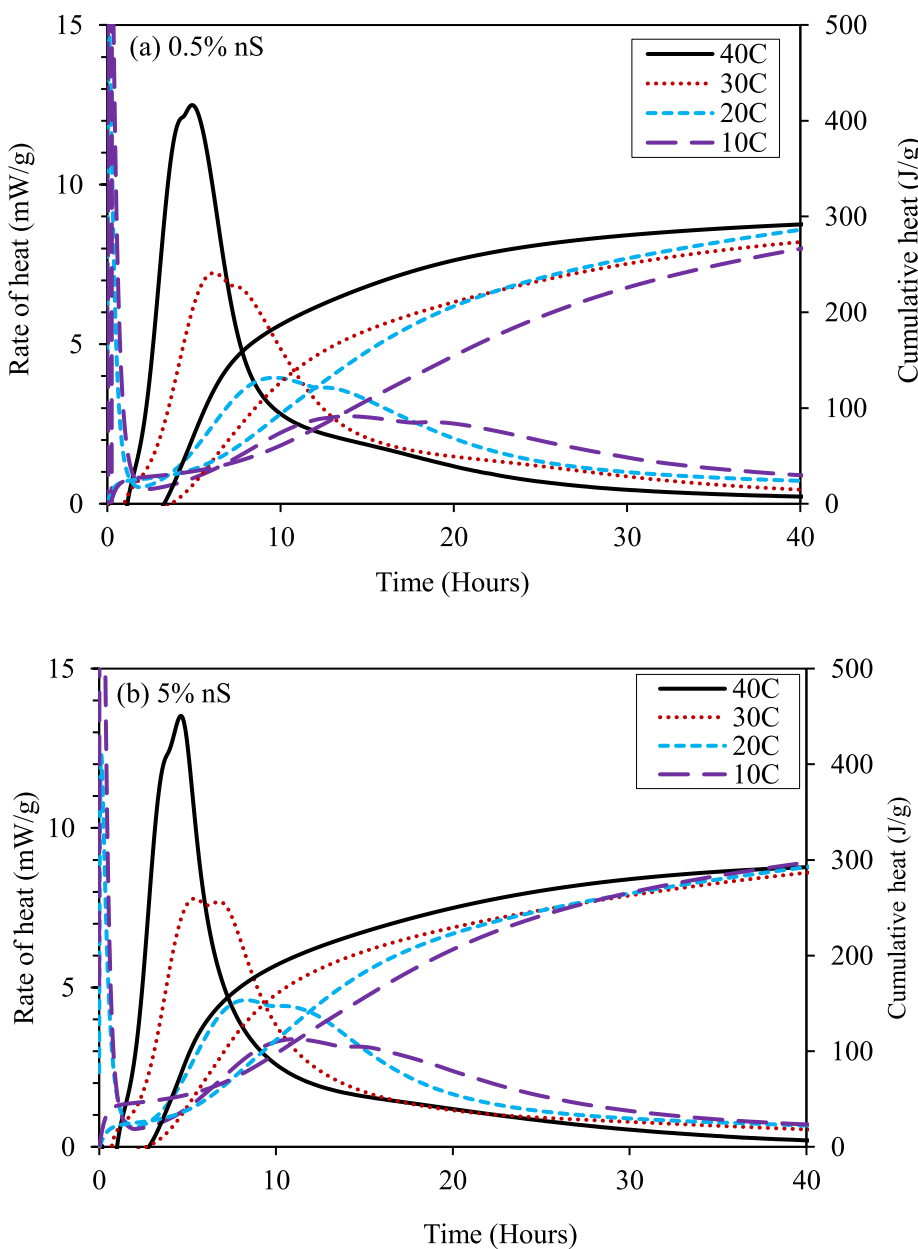


Fig. 9. Effect of temperature on the rate and cumulative heat of cement-NPs paste (Example of nS).

Table 2
Area multiplier (AM) of cement-NP pastes.

Replacement level (%)	Area Multiplier (AM)			
	nS	Col nS	nA	nL
0.0	1.00	1.00	1.00	1.00
0.5	1.44	1.50	1.22	1.11
5.0	5.63	6.21	3.32	2.16

reactions, thus improving cement hydration substantially. Other researches also concluded that nA could provide an additional source of alumina ions to the pore solution and can significantly accelerate the hydration of C₃A [9,54]. Besides, Reches et al. [64] revealed that nA could chemically react with Ca(OH)₂ to form Al(OH)₃ (bayerite/gibbsite).

(2) The relative hydration-accelerating effect of different NPs could be understood in terms of the percentage reduction in T_{Rmax} or percentage increase in S_{acc} . In general, the order of the

accelerating effect of NPs was: nS > Col nS > nA > nL. nS and Col nS, at 5% replacement, were very effective in accelerating hydration. For example, a reduction of approximately 20% in T_{Rmax} and an increment of approximately 60% in S_{acc} , were obtained at 10°C. On the other hand, even though nA increased R_{max} significantly, its impact on the acceleration of hydration was less compared to that of nS and Col nS. The accelerating-effect of nL was evident only at 5% replacement and low temperatures (10°C and 20°C).

(3) The effect of NPs on the total amount of early hydration was quantified in terms of the percentage increase in H_{24h} . In general, the order of this effect of NPs was: nS > Col nS > nA > nL. In addition to accelerating hydration, nS and Col nS were quite effective in increasing the total amount of early-age hydration as well. The corresponding effects of nA and nL were also similar to their hydration-accelerating effects.

It can be said that NPs exhibited different effects on various

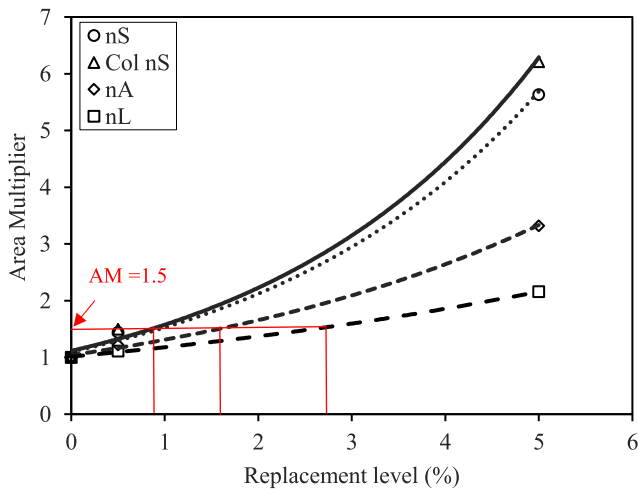


Fig. 10. Area multiplier of Portland cement for different types and replacement levels of NPs.

parameters of the hydration curve, which can be attributed to their different particle size, replacement level, testing temperature, and reactivity. These factors were combined to compare the relative effects of NPs, as presented in the next section.

3.1.4. Introduction of the concept of area multiplier (AM)

To further quantify and generalize the effect of all NPs and replacement levels, the concept of area multiplier (AM), proposed by

Tandre et al. [10], was employed. Although this concept was developed for the use of micro-sized fillers, such as limestone powder, in cement-based materials, it was applied here to compare the effect of different types of NPs on cement hydration. The AM considers the influence of the addition of a filler on the solid surface area of the cementitious system, as shown in Eq. (6) [10].

$$AM = \frac{r^* SSA_{filler}}{(100 - r)^* SSA_{cement}} \quad (6)$$

Where r (mass %) is the percentage replacement of cement by a filler (NPs in this study), and SSA_{cement} and SSA_{filler} (m^2/g) are the specific surface areas (SSA) of the cement and filler, respectively. AM is a scaling factor that describes the surface area of the filler (NP in this study) used per unit surface area of cement. For simplicity, the AM of Portland cement was assumed to be 1.0. Since NPs had much higher SSA than Portland cement (Table 1), the AM values of pastes containing NPs were higher than 1.0 (Table 2). Fig. 10 shows that AM increased exponentially with increasing NP replacement level, and SSA had a considerable impact on AM. For example, when the level of Col nS ($SSA = \sim 225 m^2/g$) replacement increased from 0.5% to 5%, the AM value of the cement system increased by a factor of approximately four. However, a corresponding increase in the replacement level of nL ($SSA = \sim 40 m^2/g$) increased the AM value by a factor of only two. It shall be noted that based on Eq. (6) AM is governed by two parameters, the SSA and the replacement level of NPs. Thus, the same AM values can be achieved for a paste containing a finer NP at a lower replacement level or containing a coarse NP at a higher replacement level. As shown in Fig. 10, AM of 1.5 could be obtained by using 0.8% Col nS, or approximately 1.7% nA, or 2.8% nL.

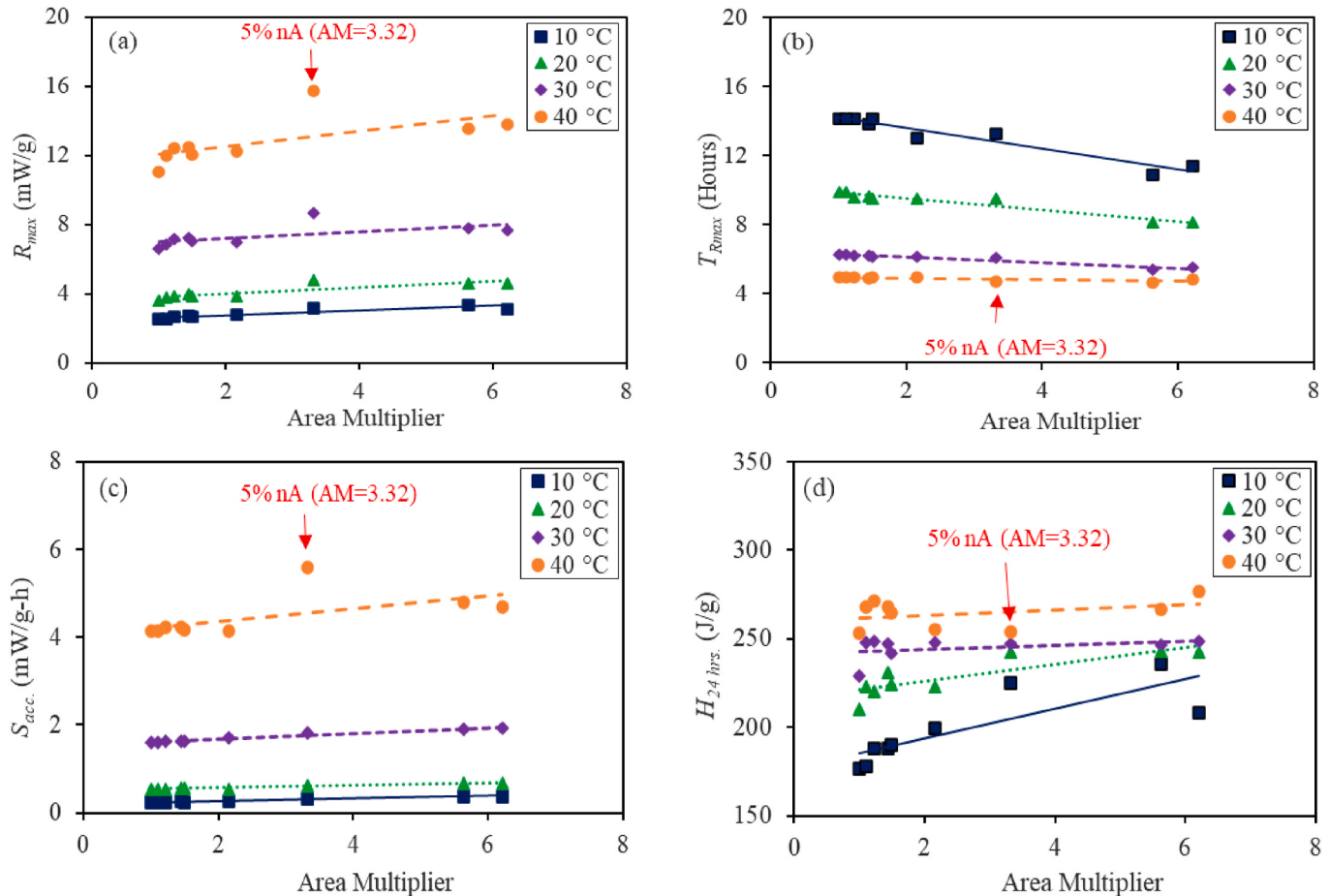
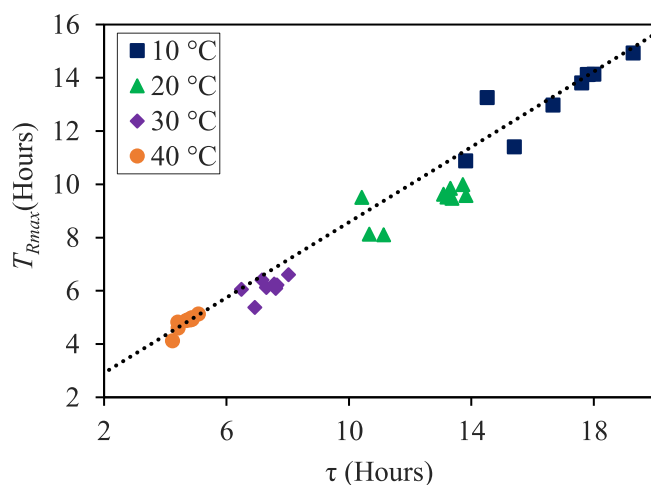


Fig. 11. Filler effect of NPs on hydration parameters explained in terms of area multiplier.

Table 3Parameters and apparent E_a determined by the modified ASTM method.

Mixture	Repl. (%)	Temp (°C)	H_u (kJ/g)	α_u	β	τ (Hours)	R^2	Apparent E_a (kJ/mol)
nS	0	10	471.36	0.690	1.168	17.79	0.994	32.54 ± 0.34
		20				13.31	0.998	
		30				7.65	0.998	
		40				4.88	0.997	
	0.5	10	472.91	0.738	1.168	17.60	0.996	33.12 ± 0.16
		20				13.09	0.998	
		30				7.61	0.999	
		40				4.69	0.998	
Col nS	0.5	10	486.79	0.695	1.119	13.82	0.996	28.29 ± 0.41
		20				10.67	0.997	
		30				6.92	0.996	
		40				4.41	0.996	
	5	10	472.91	0.723	1.165	17.82	0.996	33.04 ± 0.18
		20				13.20	0.998	
		30				7.61	0.999	
		40				4.78	0.999	
nA	0.5	10	470.15	0.745	1.150	18.00	0.995	33.24 ± 0.44
		20				13.82	0.998	
		30				7.56	0.998	
		40				4.87	0.998	
	5	10	459.29	0.731	1.084	14.52	0.996	30.67 ± 0.16
		20				10.42	0.997	
		30				6.48	0.997	
		40				4.23	0.995	
nL	0.5	10	469.01	0.741	1.179	19.28	0.996	33.31 ± 0.21
		20				13.73	0.998	
		30				8.03	0.998	
		40				5.09	0.998	
	5	10	447.79	0.749	1.191	16.67	0.996	31.78 ± 0.34
		20				13.36	0.998	
		30				7.30	0.998	
		40				4.82	0.998	

**Fig. 12.** Correlation between τ and time to reach the max. rate of heat generation.

To help further understand the effects of different NPs on the cement hydration, the AM values of the cement-NP pastes studied were plotted against four hydration curve parameters (Fig. 11). It can be observed that with increasing AM, R_{max} , S_{acc} , and $H_{24\text{ h}}$ increased, and T_{Rmax} reduced. Reduction in T_{Rmax} and increase in S_{acc} suggest that cement hydration was accelerated when a larger surface area of NPs was designated per unit surface area of cement. This could be because a higher surface area of NPs assisted in the N+G of CSH particles. Also, with increasing AM, the effect of acceleration was more prominent at

lower temperatures (10 and 20 °C). This can be substantiated by a higher slope of the best-fit lines [Fig. 11(b)] at 10 and 20 °C as compared to that at 30 and 40 °C. In general, the total amount of early-age hydration [Fig. 11(d)] also increased with increasing AM, and the increment was more at low temperatures. The formation of a higher amount of hydration products in the capillary pores might be the possible reason for the enhanced amount of early-age hydration.

As discussed previously, the same AM values can be achieved for a paste containing a finer NP at a lower replacement level or containing a coarser NP at a higher replacement level. In the present study, nS and Col nS had an SSA value of ~200 m²/g, while nL had an SSA value of only ~40 m²/g. Thus, a higher nL replacement level (3.1%) should be used to make the paste have similar calorimetric properties to the paste containing a lower Col nS replacement level (0.5%). In addition to seeding, it is generally believed that nS and Col nS could also accelerate cement hydration through their pozzolanic reaction, which consumes Ca(OH)₂, a cement hydration product, in the hydrating cement system. However, Fig. 11 shows that the data points of pastes with nS and Col nS followed the linear trend very well, indicating that the contributions to cement hydration through their pozzolanic reaction was limited when compared with the contribution of SSA at the early age of the cement hydration. Differently, in Fig. 11, the data points corresponding to AM = 3.32 (5% of nA) appear as outliers, especially at high temperatures. This was probably due to the high reactivity of nA. Even though the pastes containing 5% nA had a lower AM value (3.32) than the pastes with 5% nS (AM = 5.63) and 5% Col nS (AM = 6.21), R_{max} [Fig. 11(a)] and S_{acc} [Fig. 11(c)] values at 5% nA (at the location of AM = 3.32). Such a behavior, contrasted with the general trend of R_{max} , might be attributed to the high reactivity of nA particles in the alkaline environment of cement paste, as discussed earlier in section 3.1.3.

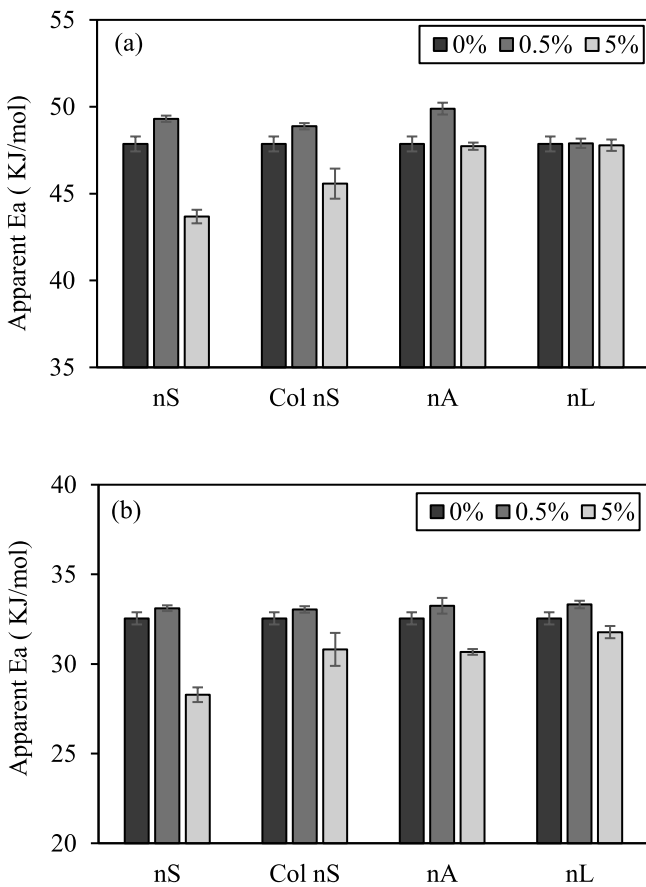


Fig. 13. Apparent E_a values from (a) linear approximation; (b) modified ASTM method.

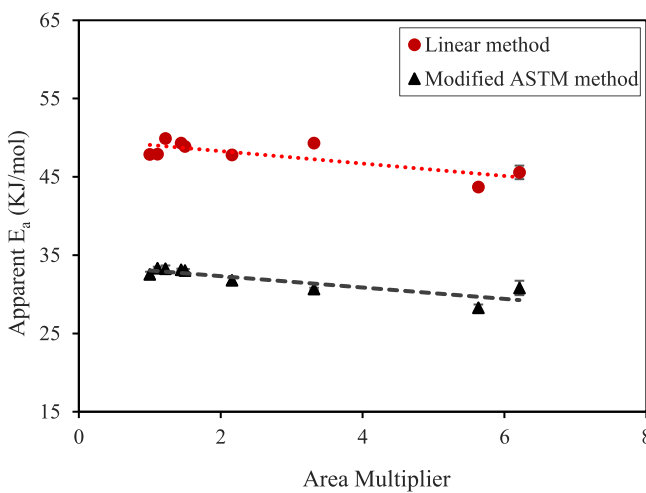


Fig. 14. Effect of area multiplier of NPs on apparent E_a of the cementitious system.

3.2. Effect of NPs on the apparent E_a of cement

3.2.1. Effect of replacement level

The apparent activation energies (E_a) of various cement-NPs combinations were calculated using the two methods described in section 2.2.3. The E_a values and other parameters obtained using the modified ASTM C1074 method are presented in Table 3. As mentioned earlier, α_u and β are independent of temperature (section 2.2.3), and their values

are the same at all four temperatures for a given paste mix. However, τ values reduced with an increase in temperature for each paste mix. Fig. 12 shows a good correlation between the τ values and the times to reach the max. rate of heat generation (T_{Rmax}) at various temperatures, a smaller τ value indicates a shorter time for a paste to reach the max. rate of heat generation, which is consistent with the observations presented earlier in section 3.1. Apparent E_a values obtained using the linear method and modified ASTM method are plotted in Fig. 13(a) and 13(b), respectively. Both figures showed a similar pattern with the change in the NP replacement levels. As the NP replacement level increased from 0% to 0.5%, apparent E_a increased slightly; however, a further increase of NP replacement level from 0.5% to 5% led to a clear reduction in apparent E_a .

To further understand the effects of various NPs, E_a calculated using the linear, and modified ASTM methods were plotted against AM, as shown in Fig. 14. Regardless of the calculation methods, the overall trend is that E_a decreased linearly with AM of pastes containing NPs. The linear relationship was very strong for E_a calculated from the ASTM method, except for the last data point (the paste containing 5% Col nS). Different from the powder NPs used, Col nS solution, as a received commercial product, possibly contain other surfactants that are not disclosed, which might have affected its E_a value. The overall decreasing trend of E_a with AM might be attributed to the following: (1) the binders with high AM had more surface area exposed for hydration reactions, (2) the additional nucleation sites provided by NPs promoted N+G in the acceleration region (stage III) of cement hydration, and (3) as more NPs, especially with a larger AM, accelerated cement hydration in stage III, cement grains were coated with more hydration products rapidly, especially at the high temperature, thus reducing the rate of diffusion-controlled hydration in stages IV-V (Figs. 4–7). However, when 0.5% NPs was used for cement replacement, their effects on cement hydration in stages IV-V were much less significant. The researchers [27,65] have suggested that the N+G-controlled process (stage III) has high E_a , whereas that of the diffusion-controlled process (stages IV-V) is low. This explains the general reduction of E_a with an increase in AM. However, more studies may be necessary to confirm these explanations.

3.2.2. Effect of NPs on equivalent age

The present study has demonstrated that the use of NPs to replace cement accelerated cement hydration more significantly at a low temperature than at a high temperature. This confirms that NP replacement for cement can help offset the delayed setting of the cement-based materials under cold weather conditions [19]. The results from the present study also indicate that the rate of cement hydration at an early age can be altered by using different types and replacement levels of NPs based on the AM value. A NP with higher SSA can function as a more effective accelerator and can be used at a small replacement level when compared with the NPs having a smaller SSA, which shall be used at a high replacement level to achieve similar effectiveness.

Another important application of apparent E_a of cement-NP mixtures is to determine concrete maturity or equivalent age. According to the ASTM C1074 [66], equivalent age is defined as the number of days or hours at a specified temperature (T_r) required to produce a maturity equal to the maturity achieved by a curing period at temperatures different from the specified temperature. The equivalent age, t_e , at a reference/specification temperature, T_r , can be determined as given in Eq. (7).

$$t_e = \sum t^* e^{-\left[-\frac{E_a}{R} \left(\frac{1}{T_i} - \frac{1}{T_r} \right) \right]} \quad (7)$$

Where T_i is the average concrete temperature during a given time period, t . Assuming $T_r = 23^\circ\text{C}$ and $T_i = 10^\circ\text{C}$ and using the apparent E_a values from Table 3 (modified ASTM method) of the control paste (no NP, $E_a = 32.54 \text{ kJ/mol}$) and the paste with 5% nS ($E_a = 28.29 \text{ kJ/mol}$), the time (t) required to attain a given equivalent age (t_e) and the

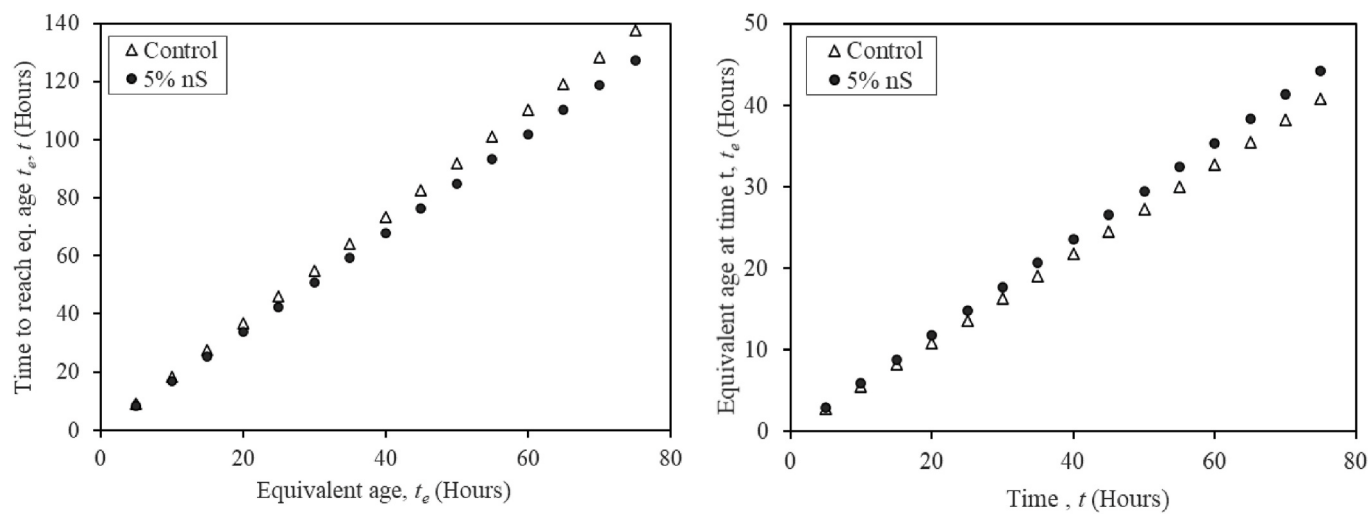


Fig. 15. Comparisons of equivalent age and the time to reach equivalent age for pastes with 0% NP (control) and 5% nS.

equivalent age (t_e) at a given time (t) can be determined according to Eq. (7). The results are presented in Fig. 15. Fig. 15(a) shows that for a given equivalent age (t_e), the paste with 5% nS reaches the equivalent age earlier; subsequently, Fig. 15(b) shows that the paste with 5% nS had a higher equivalent age at a given curing time (t). This suggests that the reduced E_a of the mixture in the presence of NPs (at high replacement level) can accelerate the setting as well as the maturity/hardening of the mixture, especially at low temperatures.

4. Conclusions

The effects of nanosized particles (NPs) on hydration kinetics and apparent activation energy (E_a) of cement pastes ($w/b = 0.45$) were evaluated. Four different types of NPs, nS, nA, and nL in a powder form, and Col nS in a liquid form, were used as cement replacement at 0.5% and 5% (by weight). The filler effect of the NPs was quantified and compared using the concept of area multiplier (AM) and with the consideration of their specific surface areas (SSA). The following conclusions can be drawn:

- (1) Regardless of their types, when NPs were used to replace Portland cement, both the max. rate of heat generation and total heat generation increased and the time to reach the max. rate of heat generation was shortened. These indicate that the NPs played a catalytic role in the reaction.
- (2) For a given type of NPs, the acceleration effect on cement hydration increased with increasing NP replacement level, but it diminished with increasing testing temperature. This suggests that the use of NPs to replace cement might be more effective for accelerating cement hydration of the cement-based materials constructed under a cold weather condition.
- (3) At the same NP replacement level, nA provided its pastes with the highest increase in the max. rate of heat generation, which might be credited to its high chemical reactivity, while nL provided pastes with the least increase in the max. rate of heat generation, which might be attributed to its relatively low SSA.
- (4) The effect of NPs on cement hydration can be understood better by using the AM factor, which describes the surface area of a type of NPs per unit surface area of cement. As the AM value of a cement system increased, more surfaces of NPs were available for the seeding of CSH nucleation. As a result, the slope of the acceleration region and the max. rate of heat generation all increased and the time to reach the max. rate of heat generation decreased linearly, reflecting a linear acceleration effect.

(5) Compared with other NPs used in this study, the pastes containing nA did not follow the linear relationships between the calorimetry parameters studied and AM. It implies that in addition to the seeding effect, the chemical reaction of nA contributed substantially to cement hydration and heat generation.

(6) NP replacement for cement slightly increased the apparent E_a of cement pastes at a low replacement level. At the same time, it noticeably reduced the apparent E_a of cement pastes at a high replacement level. This might mainly be affected by the enhanced reduction in the rate of diffusion-control hydration at high replacement levels. In general, apparent E_a reduced with an increase in AM.

CRediT authorship contribution statement

Yogiraj Sargam: Conceptualization, Experiment, Investigation, Data curation, Writing-original draft. **Kejin Wang:** Conceptualization, Resources, Funding acquisition, Supervision, Writing – review and editing.

Declaration of competing interest

The authors declare that they have no known competing financial interests or personal relationships that could have appeared to influence the work reported in this paper.

Acknowledgements

This work was derived from the project “Evaluate, Modify, and Adapt the Concrete Works Software for Iowa’s Use”, sponsored by the Iowa Highway Research Board. The authors would like to acknowledge the sponsorship. The financial support provided by the Department of Civil, Construction, and Environmental Engineering at Iowa State University is also acknowledged.

Appendix A. Supplementary data

Supplementary data to this article can be found online at <https://doi.org/10.1016/j.compositesb.2021.108836>.

References

- [1] Kong D, Huang S, Corr D, Yang Y, Shah SP. Whether do nano-particles act as nucleation sites for C-S-H gel growth during cement hydration? *Cement Concr Compos* 2018;87:98–109. <https://doi.org/10.1016/j.cemconcomp.2017.12.007>.

- [2] Camiletti J, Soliman AM, Nehdi ML. Effects of nano- and micro-limestone addition on early-age properties of ultra-high-performance concrete. *Mater Struct* 2013;46: 881–98. <https://doi.org/10.1617/s11527-012-9940-0>.
- [3] Sato T, Beaudoin JJ. Effect of nano-CaCO₃ on hydration of cement containing supplementary cementitious materials. *Adv Cement Res* 2011;23:33–43. <https://doi.org/10.1680/adcr.9.00016>.
- [4] Thomas JJ, Jennings HM, Chen JJ. Influence of nucleation seeding on the hydration mechanisms of tricalcium silicate and cement. *J Phys Chem C* 2009;113: 4327–34. <https://doi.org/10.1021/jp809811w>.
- [5] Kadri EH, Aggoun AS, De Schutter AG, Ezziane AK. Combined effect of chemical nature and fineness of mineral powders on Portland cement hydration. *Mater Struct Constr* 2010;43:665–73. <https://doi.org/10.1617/s11527-009-9519-6>.
- [6] Iskender E. Evaluation of mechanical properties of nano-clay modified asphalt mixtures. *Measurement* 2016;93:359–71. <https://doi.org/10.1016/j.measurement.2016.07.045>.
- [7] Norhasri MSM, Hamidah MS, Fadzil AM. Applications of using nano material in concrete: a review. *Construct Build Mater* 2017;133:91–7. <https://doi.org/10.1016/j.conbuildmat.2016.12.005>.
- [8] Aleem S, Abdel, Heikal M, Morsi WM. Hydration characteristic, thermal expansion and microstructure of cement containing nano-silica. *Construct Build Mater* 2014; 59:151–60. <https://doi.org/10.1016/j.conbuildmat.2014.02.039>.
- [9] Li W, Asce M, Li, Xiangyu Shu, Chen J, Long G, et al. Effects of nanoalumina and graphene oxide on early-age hydration and mechanical properties of cement paste. *J Mater Civ Eng* 2017;29:04017087. [https://doi.org/10.1061/\(ASCE\)MT.1943-5533.0001926](https://doi.org/10.1061/(ASCE)MT.1943-5533.0001926).
- [10] Tandre O, Kumar A, Bullard JW, Neithalath N, Sant G. The filler Effect : the influence of filler content and surface area on cementitious reaction rates. *J Am Ceram Soc* 2013;96:1978–90. <https://doi.org/10.1111/jace.12264>.
- [11] Gesoglu M, Güneyisi E, Asaad DS, Muhyaddin GF. Properties of low binder ultra-high performance cementitious composites: comparison of nanosilica and microsilica. *Construct Build Mater* 2016;102:706–13. <https://doi.org/10.1016/j.conbuildmat.2015.11.020>.
- [12] Ghafari E, Costa H, Júlio E, Portugal A, Durães L. The effect of nanosilica addition on flowability, strength and transport properties of ultra high performance concrete. *Mater Des* 2014;59:1–9. <https://doi.org/10.1016/j.matdes.2014.02.051>.
- [13] Jo B-W, Kim C-H, Tae G, Park J-B. Characteristics of cement mortar with nano-SiO₂ particles. *Construct Build Mater* 2007;21:1351–5. <https://doi.org/10.1016/j.conbuildmat.2005.12.020>.
- [14] Nazari A, Riahi S. The effects of SiO₂ nanoparticles on physical and mechanical properties of high strength compacting concrete. *Compos B Eng* 2011;42:570–8. <https://doi.org/10.1016/j.compositesb.2010.09.025>.
- [15] Rong Z, Sun W, Xiai H, Jiang G. Effects of nano-SiO₂ particles on the mechanical and microstructural properties of ultra-high performance cementitious composites. *Cement Concr Compos* 2015;56:25–31. <https://doi.org/10.1016/j.cemconcomp.2014.11.001>.
- [16] Senff L, Hotza D, Repette WL, Ferreira VM, Labrincha JA. Mortars with nano-SiO₂ and micro-SiO₂ investigated by experimental design. *Construct Build Mater* 2010; 24:1432–7. <https://doi.org/10.1016/j.conbuildmat.2010.01.012>.
- [17] Zhang L, Ma N, Wang Y, Han B, Cui X, Yu X, et al. Study on the reinforcing mechanisms of nano silica to cement-based materials with theoretical calculation and experimental evidence. *J Compos Mater* 2016;50:4135–46. <https://doi.org/10.1177/0021998316632602>.
- [18] Korayem AH, Tourani N, Zakertabrizi M, Sabziparvar AM, Duan WH. A review of dispersion of nanoparticles in cementitious matrices: nanoparticle geometry perspective. *Construct Build Mater* 2017;153:346–57. <https://doi.org/10.1016/j.conbuildmat.2017.06.164>.
- [19] Bentz DP. Activation energies of high-volume fly ash ternary blends: hydration and setting. *Cement Concr Compos* 2014;53:214–23. <https://doi.org/10.1016/j.cemconcomp.2014.06.018>.
- [20] Sargam Y, Faytarouni M, Riding K, Wang K, Jahren C, Shen J. Predicting thermal performance of a mass concrete foundation - a field monitoring case study. *Case Stud Constr Mater* 2019;11:e00289. <https://doi.org/10.1016/j.cscm.2019.e00289>.
- [21] Sargam Y, Wang K, Alleman JE. Effect of modern concrete materials on thermal conductivity. *J Mater Civ Eng* 2020;32:04020058. [https://doi.org/10.1061/\(ASCE\)MT.1943-5533.0003026](https://doi.org/10.1061/(ASCE)MT.1943-5533.0003026).
- [22] Kada-Benameur H, Wirquin E, Duthoit B. Determination of apparent activation energy of concrete by isothermal calorimetry. *Cement Concr Res* 2000;30:301–5. [https://doi.org/10.1016/S0008-8846\(99\)00250-1](https://doi.org/10.1016/S0008-8846(99)00250-1).
- [23] D 'aloia L, Chanvillard G. Determining the "apparent" activation energy of concrete E a —numerical simulations of the heat of hydration of cement. *Cement Concr Res* 2002;32:1277–89.
- [24] Poole J L, Riding K A, Folliard K J, Juenger M CG, Schindler A K. Methods for calculating activation energy for portland cement. *ACI Mater J* 2007;104:303.
- [25] Riding KA, Poole JL, Folliard KJ, Juenger MCG, Schindler AK. New model for estimating apparent activation energy of cementitious systems. *ACI Mater J* 2011; 108.
- [26] Thomas JJ. The instantaneous apparent activation energy of cement hydration measured using a novel calorimetry-based method. *J Am Ceram Soc* 2012;95: 3291–6. <https://doi.org/10.1111/j.1551-2916.2012.05396.x>.
- [27] Ma W, Sample D, Martin R, Brown PW, Ma R, Martin W, et al. Calorimetric study of cement blends containing fly ash, silica fume, and slag at elevated temperatures. *Cem Concr Aggregates* 1994;16:93–9.
- [28] Lavergne F, Belhadi R, Carriat J, Ben Fraj A. Effect of nano-silica particles on the hydration, the rheology and the strength development of a blended cement paste. *Cement Concr Compos* 2019;95:42–55. <https://doi.org/10.1016/j.cemconcomp.2018.10.007>.
- [29] Liu X, Chen L, Liu A, Wang X. Effect of nano-CaCO₃ on properties of cement paste. *Energy Procedia* 2012;16:991–6. <https://doi.org/10.1016/j.egypro.2012.01.158>.
- [30] Kong D, Corr DJ, Hou P, Yang Y, Shah SP. Influence of colloidal silica sol on fresh properties of cement paste as compared to nano-silica powder with agglomerates in micron-scale. *Cement Concr Compos* 2015;63:30–41. <https://doi.org/10.1016/j.cemconcomp.2015.08.002>.
- [31] Senff L, Labrincha JA, Ferreira VM, Hotza D, Repette WL. Effect of nano-silica on rheology and fresh properties of cement pastes and mortars. *Construct Build Mater* 2009;23:2487–91. <https://doi.org/10.1016/j.conbuildmat.2009.02.005>.
- [32] Güneyisi E, Gesoglu M, Al-Goody A, Ipek S. Fresh and rheological behavior of nano-silica and fly ash blended self-compacting concrete. *Construct Build Mater* 2015;95:29–44. <https://doi.org/10.1016/j.conbuildmat.2015.07.142>.
- [33] Kong D, Pan H, Wang L, Corr DJ, Yang Y, Shah SP, et al. Effect and mechanism of colloidal silica sol on properties and microstructure of the hardened cement-based materials as compared to nano-silica powder with agglomerates in micron-scale. *Cement Concr Compos* 2019;98:137–49. <https://doi.org/10.1016/j.cemconcomp.2019.02.015>.
- [34] Barbhuiya S, Mukherjee S, Nikraz H. Effects of nano-Al₂O₃ on early-age microstructural properties of cement paste. *Construct Build Mater* 2014;52: 189–93. <https://doi.org/10.1016/j.conbuildmat.2013.11.010>.
- [35] Li H, Xiao HG, Yuan J, Ou J. Microstructure of cement mortar with nano-particles. *Compos B Eng* 2004;35:185–9. [https://doi.org/10.1016/S1359-8368\(03\)00052-0](https://doi.org/10.1016/S1359-8368(03)00052-0).
- [36] Ji T. Preliminary study on the water permeability and microstructure of concrete incorporating nano-SiO₂. *Cement Concr Res* 2005;35:1943–7. <https://doi.org/10.1016/j.cemconres.2005.07.004>.
- [37] Shekari AH, Razzaghi MS. Influence of nano particles on durability and mechanical properties of high performance concrete. *Procedia Eng* 2011;14:3036–41. <https://doi.org/10.1016/j.proeng.2011.07.382>.
- [38] Li Z, Wang H, He S, Lu Y, Wang M. Investigations on the preparation and mechanical properties of the nano-alumina reinforced cement composite. *Mater Lett* 2006;60:356–9. <https://doi.org/10.1016/j.matlet.2005.08.061>.
- [39] Morsy MS, Alsayed SH, Aqel M. Hybrid effect of carbon nanotube and nano-clay on physico-mechanical properties of cement mortar. *Construct Build Mater* 2011;25: 145–9. <https://doi.org/10.1016/j.conbuildmat.2010.06.046>.
- [40] Naji Givi A, Abdul Rashid S, Aziz FNA, Salleh MAM. Experimental investigation of the size effects of SiO₂ nano-particles on the mechanical properties of binary blended concrete. *Compos B Eng* 2010;41:673–7. <https://doi.org/10.1016/j.compositesb.2010.08.003>.
- [41] Meng T, Yu Y, Qian X, Zhan S, Qian K. Effect of nano-TiO₂ on the mechanical properties of cement mortar. *Construct Build Mater* 2012;29:241–5. <https://doi.org/10.1016/j.conbuildmat.2011.10.047>.
- [42] Aly M, Hashmi MSJ, Olabi AG, Messeiry M, Abadir EF, Hussain AI. Effect of colloidal nano-silica on the mechanical and physical behaviour of waste-glass cement mortar. *Mater Des* 2012;33:127–35. <https://doi.org/10.1016/j.matdes.2011.07.008>.
- [43] Du H, Du S, Liu X. Durability performances of concrete with nano-silica. *Construct Build Mater* 2014;73:705–12. <https://doi.org/10.1016/j.conbuildmat.2014.10.014>.
- [44] Wilben S, Supti M, Uddin F, Shaikh A. Durability properties of high volume fly ash concrete containing nano-silica. *Mater Struct* 2015;48:2431–45. <https://doi.org/10.1617/s11527-014-0329-0>.
- [45] Zhang MH, Li H. Pore structure and chloride permeability of concrete containing nano-particles for pavement. *Construct Build Mater* 2011;25:608–16. <https://doi.org/10.1016/j.conbuildmat.2010.07.032>.
- [46] Kong D, Huang S, Corr D, Yang Y, Shah SP. Whether do nano-particles act as nucleation sites for C-S-H gel growth during cement hydration? *Cement Concr Compos* 2018;87:98–109. <https://doi.org/10.1016/j.cemconcomp.2017.12.007>.
- [47] Jayapalan AR, Lee BY, Kurtis KE. Can nanotechnology be "green"? Comparing efficacy of nano and microparticles in cementitious materials. *Cement Concr Compos* 2013;36:16–24. <https://doi.org/10.1016/j.cemconcomp.2012.11.002>.
- [48] Zhang M-H, Islam J, Peethamparan S. Use of nano-silica to increase early strength and reduce setting time of concretes with high volumes of slag. *Cement Concr Compos* 2012;34:650–62. <https://doi.org/10.1016/j.cemconcomp.2012.02.005>.
- [49] Zhou J, Zheng K, Liu Z, He F. Chemical effect of nano-alumina on early-age hydration of Portland cement. *Cement Concr Res* 2019;116:159–67. <https://doi.org/10.1016/j.cemconres.2018.11.007>.
- [50] Wang X, Wang K, Tanesi J, Ardani A, Wang R. Effects of nanomaterials on the hydration kinetics and rheology of portland cement pastes advances in Civil engineering materials. *Adv Civ Eng Mater* 2014;3:142–59. <https://doi.org/10.1520/ACEM20140021>.
- [51] Jayapalan AR, Jue ML, Kurtis KE. Nanoparticles and apparent activation energy of Portland cement. *J Am Ceram Soc* 2014;97:1534–42. <https://doi.org/10.1111/jace.12878>.
- [52] ASTM C150/C150M-18. Standard specification for portland cement. West Conshohocken, PA, https://doi.org/10.1520/C0150_C0150M-18; 2018.
- [53] ASTM C1679. Standard practice for measuring hydration kinetics of hydraulic cementitious mixtures using isothermal calorimetry. 2017. West Conshohocken, PA.
- [54] Bullard JW, Jennings HM, Livingston RA, Nonat A, Scherer GW, Schweitzer JS, et al. Mechanisms of cement hydration. *Cement Concr Res* 2011;41:1208–23. <https://doi.org/10.1016/j.cemconres.2010.09.011>.
- [55] Garrault S, Nonat A. Hydrated layer formation on tricalcium and dicalcium silicate surfaces: experimental study and numerical simulations. *Langmuir* 2001;17: 8131–8. <https://doi.org/10.1021/la011201z>.

- [56] Bishnoi S, Scrivener KL. Studying nucleation and growth kinetics of alite hydration using mic. *Cement Concr Res* 2009;39:849–60. <https://doi.org/10.1016/j.cemconres.2009.07.004>.
- [57] Van Breugel K. Prediction of temperature development in hardening concrete. *RILEM Rep* 15 Prev Therm Crack Concr Early Ages 1998;15:51–75.
- [58] De Schutter G, Taerwe L. Degree of hydration-based description of mechanical properties of early age concrete. *Mater Struct* 1996;29:335. <https://doi.org/10.1007/BF02486341>.
- [59] Waller V, De LArrard F, Roussel P. Modeling the temperature rise in massive HPC structures. In: Fourth Int. Symp. Util. High strength/high Perform. Concr. Paris, France: TOC; 1996.
- [60] Xu Q, Hu J, Ruiz JM, Wang K, Ge Z. Isothermal calorimetry tests and modeling of cement hydration parameters. *Thermochim Acta* 2010;499:91–9. <https://doi.org/10.1016/j.tca.2009.11.007>.
- [61] Kjellsen KO, Detwiler RJ. Reaction kinetics of portland cement mortars hydrated at different temperatures. *Cement Concr Res* 1992;22:112–20. [https://doi.org/10.1016/0008-8846\(92\)90141-H](https://doi.org/10.1016/0008-8846(92)90141-H).
- [62] Thomas JJ. A new approach to modeling the nucleation and growth kinetics of tricalcium silicate hydration. *J Am Ceram Soc* 2007;90:3282–8. <https://doi.org/10.1111/j.1551-2916.2007.01858.x>.
- [63] Zhan BJ, Xuan DX, Poon CS. The effect of nanoalumina on early hydration and mechanical properties of cement pastes. *Construct Build Mater* 2019;202:169–76. <https://doi.org/10.1016/j.conbuildmat.2019.01.022>.
- [64] Reches Y, Thomson K, Helbing M, Kosson DS, Sanchez F. Agglomeration and reactivity of nanoparticles of SiO₂, TiO₂, Al₂O₃, Fe₂O₃, and clays in cement pastes and effects on compressive strength at ambient and elevated temperatures. *Construct Build Mater* 2018;167:860–73. <https://doi.org/10.1016/j.conbuildmat.2018.02.032>.
- [65] Thomas JJ, Jennings HM. Effects of D₂O and mixing on the early hydration kinetics of tricalcium silicate. *Chem Mater* 1999;11:1907–14. <https://doi.org/10.1021/cm9900857>.
- [66] ASTM C1074. Estimating concrete strength by the maturity method. West Conshohocken, PA, <https://doi.org/10.1520/C1074-11.2>; 2015.